

Temperature dependence of the radiative lifetime in GaN

Oliver Brandt, Jens Ringling, and Klaus H. Ploog

Paul-Drude-Institut für Festkörperelektronik, Hausvogteiplatz 5-7, D-10117 Berlin, Germany

Hans-Jürgen Wünsche and Fritz Henneberger

Humboldt-Universität zu Berlin, Institut für Physik, Invalidenstrasse 110, D-10115 Berlin, Germany

(Received 8 September 1998)

Using time-resolved photoluminescence spectroscopy, we determine the temperature dependence of the radiative lifetime for GaN layers with doping levels from 10^{16} to 10^{18} cm^{-3} . The experimental results are analyzed by a coupled rate-equation model taking into account band-to-band, free and bound excitons, as well as donor-to-band recombination. An analytic expression for the radiative lifetime of this coupled system is derived and fit to the data. Over the entire temperature range, radiative recombination is strongly affected by the decay of either bound or free excitons. The temperature dependence and the absolute values for the radiative lifetime are governed by the coupling between the individual populations. This coupling in turn is determined by the binding energies of the respective species. Using a binding energy of 26.4 meV for the free exciton, we obtain best-fit values of 30 ± 6 and 36.3 ± 2 meV for the donor and the donor-bound exciton, respectively. [S0163-1829(98)50648-0]

Radiative recombination in semiconductors may occur by several mechanisms. The lowest energy state in an ideal crystal is the free exciton-polariton, which, in principle, does not decay because of momentum conservation.¹⁻³ The actual exciton-polariton lifetime is thus determined by scattering with phonons, impurities, and surfaces.¹ At low temperatures, however, the exciton may instead be captured by the impurities, and bound exciton transitions will then dominate recombination. At high temperatures, the polariton character of the exciton is gradually washed out, and it becomes as active in recombination as expected from a semiclassical point of view.^{1,4} However, band-to-band transitions now compete with exciton recombination and gradually take over for kT exceeding the exciton binding energy.

In an idealized semiconductor containing only one kind of impurity, we have thus to consider (at least) four coupled recombination channels: band-to-band, free exciton, bound exciton, and impurity-to-band. Provided that these channels are spectrally distinct, one can monitor both relaxation and recombination processes of the coupled system using time-resolved photoluminescence (PL) spectroscopy. The spectral separation of these transitions is, however, in the range of a few meV, and at high temperatures they will not be resolvable. This is true even for wide-gap semiconductors such as GaN, where the free and bound exciton as well as the shallow donor state all lie within an energy interval of at most 15 meV.⁵ For most GaN layers the reported PL linewidths are on the same order even at low temperature.³ *The measured radiative lifetime is then a composite of the individual lifetimes of each of the above mentioned transitions, and not a unique lifetime specific for the material system.*

In this paper, we study both experimentally and theoretically the temperature dependence of the radiative lifetime in GaN. The samples under investigation are grown on *n*-type Si-terminated 6H-SiC(0001) substrates either by plasma-assisted molecular beam epitaxy (MBE) or by low-pressure metal-organic vapor phase epitaxy (MOVPE).⁷ The samples

differ in their thickness and buffer layer sequence, but, most importantly, in their residual doping level measured by capacitance voltage (CV), which ranges from low 10^{16} cm^{-3} for the MOVPE samples (#3 and #4) to mid 10^{17} cm^{-3} (#2) and low 10^{18} cm^{-3} (#1) for the MBE samples. Samples #1 and #2 consist of a 0.52 and 0.3 μm GaN layer, respectively, deposited directly onto the substrate. Sample #3 consists of a 0.5 μm GaN layer with a 0.5 μm (AlGa)N buffer layer, while sample #4 contains a 1.3 μm GaN layer with a 10 nm AlN buffer layer. The radiative lifetime is determined by time-resolved PL spectroscopy. The measurements are performed using a frequency-tripled Ti:sapphire laser with a pulse width of 150 fs and a syncroscan streak-camera system. The excitation energy and fluence are set to 4.96 eV and 1 mJ/cm^2 , respectively. The overall temporal resolution of this setup is 2 ps.

Figure 1 shows the cw PL spectra of three of the samples at 5 K. The different doping levels of these samples manifest

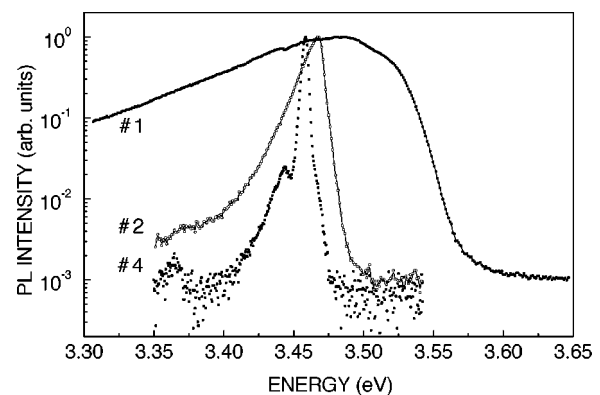


FIG. 1. Logarithmic display of the PL spectra of samples #1, #2, and #4 at 5 K. Note the drastically different linewidths and the absence of any structure in all spectra (the sharp peak at 3.447 eV in the spectrum of sample #4 is due to the outgoing resonance with the free-exciton state for fourth-order Raman scattering).

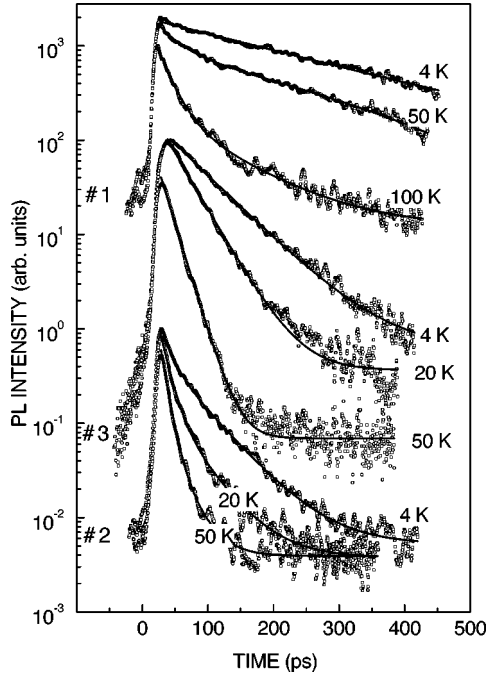


FIG. 2. PL transients of samples #1, #2, and #3 at different temperatures as indicated in the figure. The points are the experimental data, while the solid lines show mono- or biexponential fits to them. The spectra of different samples are vertically offset for clarity. For each sample, the decrease in peak intensity with temperature directly corresponds to an increasing radiative lifetime.

themselves most evidently in their different PL line shape and linewidth. While the linewidth is about 4–6 meV for samples with a doping level around 10^{16} cm^{-3} , it increases to 15–20 meV for samples in the mid 10^{17} cm^{-3} range and to above 100 meV for samples approaching degenerate doping ($2 \times 10^{18} \text{ cm}^{-3}$). Simultaneously, the PL peak position shifts to higher energy. The excessive broadening of the low-energy tail is consistent with impurity-band formation and band tailing,⁸ while the comparatively abrupt high-energy cutoff together with the pronounced blueshift is evidence for non- \mathbf{k} conserving transitions involving the Fermi edge (Burstein-Moss effect in emission).⁸ Most important, however, is the complete absence of any discernable structure in all of these spectra. For any further analysis, we have to assume that the observed PL line represents a superposition of several transitions as already mentioned in the introduction.

In Fig. 2, we show the PL transients of three of the samples at different temperatures. The measured decay times are, in general, too short to be ascribed to radiative processes only except for sample #1, which exhibits a decay time of about 250 ps between 5 and 30 K. It is furthermore interesting to note that most of these transients cannot be described by a monoexponential, but rather by a biexponential decay. Biexponential decays are characteristic of capture processes in a multilevel system, and may here be interpreted as being due to the capture to deeper (nonradiative) centers either in the bulk or at the surface/interface of the layer.⁹ In any case, when analyzing the decay time in the standard way,¹⁰ namely, by taking $\tau_{\text{PL}}(T) = [1/\tau_r(T) + 1/\tau_{\text{nr}}(T)]^{-1}$, where τ_{nr} includes all possible nonradiative contributions, and $I_{\text{PL}}(T) = \eta_{\text{PL}}(T)I_{\text{PL}}(0)$, with $\eta_{\text{PL}}(T) = \tau_{\text{PL}}/\tau_r$, the question

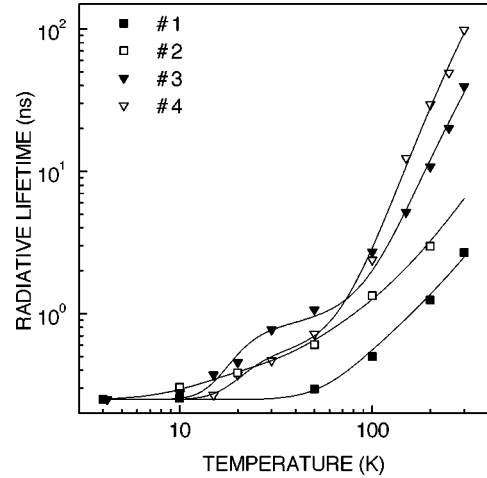


FIG. 3. Measured (symbols) and calculated (lines) radiative lifetimes vs temperature for samples #1 to #4 as indicated in the figure.

arises which value should be used for τ_{PL} in the case of a biexponential decay. We circumvent this ambiguity here by noting that the radiative decay rate is equal to the peak intensity of the transient divided by the incident fluence provided that the duration of the exciting pulse is much shorter than any recombination process in the sample.¹¹ Since we do not measure the PL intensity in absolute units, this procedure requires assigning a value for τ_r at the lowest temperature (note that this is equivalent to the standard procedure where a value for η_{PL} is required). Since the emission of GaN at low temperatures is dominated by bound excitons, we set the radiative lifetime at 4 K to 250 ps, which is the value calculated for GaN in the frame of Rashba's treatment.¹²

Figure 3 displays the radiative lifetimes thus obtained as well as fits to the data (see below) for all samples. There is a clear trend toward longer lifetimes with decreasing doping levels, as expected for, e.g., band-to-band-transitions. However, the radiative recombination coefficient B for GaN is only $4.4 \times 10^{-11} \text{ cm}^3/\text{s}$ at 300 K,¹³ resulting in a band-to-band lifetime of 2.3 μs at a doping level of 10^{16} cm^{-3} . Qualitatively, the rather short lifetimes measured even for samples #3 and #4 evidence the participation of excitons up to room temperature. The subtle differences between the samples at lower temperatures are, however, beyond the reach of qualitative considerations.

For quantitatively understanding the measured temperature dependence of the radiative lifetime, we finally perform a theoretical analysis based on a rate-equation model for the major recombination channels in GaN. The temporal evolution of the concentration of electrons ($n = n_0 + \Delta n$), holes ($p = \Delta p$), free (n_x) and bound (n_b) excitons, and occupied donors (N_D^0), is governed by the following coupled set of differential equations:

$$dn/dt = -Bnp + d_x n_x - f_x np - c_r n N_D^+ + c_e N_D^0, \quad (1)$$

$$dp/dt = -Bnp + d_x n_x - f_x np - b_D p N_D^0, \quad (2)$$

$$dn_x/dt = -\gamma_x n_x - b_r n_x N_D^0 + b_e n_b - d_x n_x + f_x np, \quad (3)$$

$$dn_b/dt = -\gamma_b n_b + b_r n_x N_D^0 - b_e n_b, \quad (4)$$

$$dN_D^0/dt = -b_{DP}N_D^0 + c_r n N_D^+ - c_e N_D^0 - b_r n_x N_D^0 + b_e n_b + \gamma_b n_b. \quad (5)$$

The first terms of these equations account for radiative recombination. The following terms describe the formation (f_x) and dissociation (d_x) of free excitons, the capture (b_r) and emission (b_e) of a free exciton by a neutral donor, and the capture (c_r) and emission (c_e) of an electron by a charged and neutral donor, respectively. Together with these equations, it is required that

$$N_D = N_D^0 + N_D^+ + n_b, \quad (6)$$

where N_D is the total donor concentration in the layer, and

$$n = p + N_D^+, \quad (7)$$

accounting for charge conservation. Note that N_D^+ is equal to the background doping n_0 only in equilibrium, but not necessarily under transient conditions.

While it is straightforward to formulate Eqs. (1)–(5), their solution is difficult both physically and numerically. All of the six capture coefficients are, essentially, unknown, and their determination remains a formidable challenge for both experiment and theory. All we know is that capture processes in semiconductors tend to be very much faster than recombination processes. This fact has an important consequence: *the individual populations of all levels decay with a common lifetime*. It also, however, causes the above system of differential equations to be stiff, in that the slow process of interest disappears in the numerical noise following the initial, rapid process.

The solution of both of these obstacles lies in the experimental finding of PL lines which, when spectrally integrated, represent the sum of Eqs. (2)–(4) [or alternatively, of Eqs. (1), (3)–(5)]. First of all, we may eliminate three of the unknown coefficients by utilizing detailed balance between capture and emission processes, yielding $f_x/d_x = \sigma_x = 2(E_x/Ry)\exp(E_x/kT)/N_{cv}$, $b_r/b_e = \sigma_b = 2\exp(aE_d/kT)/N_f$, and $c_r/c_e = \sigma_d = 2\exp(E_d/kT)/N_c$, where Ry and $E_x = Ry/[1 + n/(2n_M)]$ are the exciton binding energies for vanishing and finite carrier concentration, respectively, with the Mott density $n_M = 2.2 \times 10^{17} \text{ cm}^{-3}$.¹³ E_d denotes the donor binding energy, and a the fraction of E_d transferred to a bound exciton. N_{cv} , N_f , and N_c are the effective reduced, exciton, and conduction-band densities of states, respectively. Next, we sum up Eqs. (2)–(4) which contain the minority carrier processes, and express the dynamic variables as functions of n only by assuming that quasistationary conditions for all relaxation processes are established.^{13,14} *This procedure eliminates all explicit capture terms*. The resulting equation reads

$$dn/dt = -Z/(N + \rho P), \quad (8)$$

where

$$Z = \left[B + \sigma_x \gamma_x + \frac{\sigma_b \sigma_x \gamma_b (N_D - n + p)}{1 + \sigma_b \sigma_x n p} + \frac{b_d (N_D - n + p)}{n(1 + \sigma_b \sigma_x n p)} \right] n p, \quad (9)$$

$$N = \sigma_x p + \sigma_b \sigma_x \left[\frac{p(N_D - n + p)}{(1 + \sigma_b \sigma_x n p)^2} - \frac{np}{1 + \sigma_b \sigma_x n p} \right], \quad (10)$$

$$\rho = \frac{1 + \sigma_d [1 + 2\sigma_b \sigma_x n p (n - p)] + n(1 + \sigma_b \sigma_x n p)}{1 - \sigma_d [\sigma_b \sigma_x n^2 (n - p) - n(1 + \sigma_b \sigma_x n p)]}, \quad (11)$$

$$P = 1 + \sigma_x n + \sigma_b \sigma_x \left[\frac{n(N_D - n + p)}{(1 + \sigma_b \sigma_x n p)^2} + \frac{np}{1 + \sigma_b \sigma_x n p} \right], \quad (12)$$

with

$$p = \frac{r}{2} (\sqrt{1 + s(2/r)^2} - 1), \quad (13)$$

where

$$r = \frac{1 + \sigma_d n (1 - \sigma_b \sigma_x n^2)}{\sigma_b \sigma_x \sigma_d n^2}, \quad (14)$$

$$s = \frac{n + \sigma_d n^2 - N_D}{\sigma_b \sigma_x \sigma_d n^2}. \quad (15)$$

Since we are interested in an actual (time-independent) lifetime, we finally consider the case of $\Delta n \ll n_0$, which is also realized in our experiments. For this condition, Eq. (8) reduces to $dn/dt = -\gamma_{\text{eff}} n$ with the common radiative decay rate of the coupled system

$$\gamma_{\text{eff}} = \gamma_c \frac{1 + \sigma_x n_0 [\gamma_x / \gamma_c + \sigma_b (N_D - n_0) (\gamma_b / \gamma_c)] + \gamma_d / \gamma_c}{1 + \sigma_x n_0 [1 + \sigma_b (N_D - n_0)]}, \quad (16)$$

where $\gamma_c = B n_0$ and $\gamma_d = b_d (N_D - n_0)$. It is easily seen that this expression indeed mediates between the limits $\gamma_{\text{eff}} \rightarrow \gamma_b$ for $T \rightarrow 0$ and $\gamma_{\text{eff}} \rightarrow \gamma_c$ for $T \rightarrow \infty$. Note that these limits are independent of the magnitude of the other rates, contrary to the case of uncoupled systems decaying in parallel, where the rates simply add. Being thus confident that Eq. (16) is a sensible approximation, we finally fit it to the experimental data shown in Fig. 3.

The radiative rates and recombination coefficients have been determined via the relation between oscillator strength and radiative rate¹⁵ and the van Roosbroeck–Shockley relation,^{4,13} respectively. The free parameters of first order in Eq. (16) are a , E_d , and N_D , the latter of which is separated in a temperature-activated fraction given by $n_0 = (\sqrt{1 + 4\sigma_d N_D} - 1)/2\sigma_d$ and a constant to account for impurity-band formation at higher doping levels. Since γ_x has been derived semiclassically, it approaches unphysically short values for low temperatures, causing the calculated lifetime to have a (shallow) minimum. For improving the fit, we thus add two free parameters of second order which account for the polariton character by allowing the exciton lifetime to saturate or even increase with decreasing temperature. Note that, in contrast to a previous work,¹⁰ we do not treat the exciton binding energy as a fit parameter which is assumed here to be 26.4 meV.

The fits obtained are in very satisfactory agreement with the experimental data (see Fig. 3) and return physically reasonable values for the fitting parameters. Unique fits are ob-

tained for samples #3 and #4, yielding values of $a=0.21 \pm 0.06$, $E_d=30 \pm 6$ meV, and a total donor concentration of 5.6×10^{16} and 1.9×10^{16} cm⁻³, respectively. About 25% of this concentration is not activated. In contrast, for samples #1 and #2 total concentrations of 5.6×10^{17} and 1.8×10^{18} cm⁻³, respectively, are obtained, with a nonactivated fraction of over 50%. For both of these samples, a is about 0.1 and E_d about 18 meV, but with a considerably larger error margin than for samples #3 and #4. Whether the lower values for a and E_d are due to different donor species or a result of donor-band formation at these high doping levels cannot be decisively answered. In any case, the values obtained are well within the range determined by other means.⁵ Finally, the phenomenological correction for the exciton lifetime turns out to be an essentially constant offset of about 500 ps for all samples, meaning that the polariton character of the exciton takes over at temperatures below 50 K.

Finally, the fits allow us to determine the relative contribution of the individual recombination channels. At low temperature, (<20 K) recombination is governed by bound excitons for all samples. Between 20 and 50 K, the bound

excitons largely dissociate, and free exciton recombination becomes dominant. The coupling between free excitons and free carriers is important already at intermediate temperature (100 K) and determines the slope of the radiative lifetime with further increasing temperature. Note, however, that the radiative decay rate is substantially enhanced by the excitonic contribution even at room temperature. In particular, the free exciton transition would spectrally dominate at room temperature for all samples but sample #1, for which screening by the high electron background largely diminishes the free exciton decay rate. Correspondingly, donor-to-band transitions are of minor importance for all samples but sample #1, for which they constitute a significant contribution at intermediate and higher temperatures (100–300 K).

We are indebted to Bin Yang for MBE growth and Jürgen Off (Universität Stuttgart) for MOVPE growth. We furthermore thank Holger Grahn, Patrick Waltereit, and Ferdinand Scholz (Universität Stuttgart) for valuable discussions and critical reading of the manuscript. Furthermore, we acknowledge partial financial support of this work by the Deutsche Forschungsgemeinschaft.

¹J. J. Hopfield, Phys. Rev. **112**, 1555 (1958).

²L. C. Andreani and A. Pasquarello, Phys. Rev. B **42**, 8928 (1990).

³S. Pau, Z. X. Liu, J. Kuhl, J. Ringling, H. T. Grahn, M. A. Kahn, C. J. Sun, O. Ambacher, and M. Stutzmann, Phys. Rev. B **57**, 7066 (1998).

⁴H. B. Bebb and E. W. Williams, in *Semiconductors and Semimetals*, edited by R. K. Willardson and A. C. Beer (Academic Press, London, 1972), Vol. 8.

⁵S. Fischer, D. Volm, D. Kovalev, B. Averboukh, A. Graber, H. C. Alt, and B. K. Meyer, Mater. Sci. Eng., B **43**, 192 (1997).

⁶B. Yang, O. Brandt, A. Trampert, B. Jenichen, and K. H. Ploog, Appl. Phys. Lett. (to be published).

⁷J. Off and F. Scholz (unpublished).

⁸E. Iliopoulos, D. Doppelapudi, H. M. Ng, and T. D. Moustakas, Appl. Phys. Lett. **73**, 375 (1998).

⁹O. Brandt, B. Yang, H.-J. Wünsche, U. Jahn, J. Ringling, G. Paris, H. T. Grahn, and K. H. Ploog, Phys. Rev. B **58**, 13 407 (1998).

¹⁰J. S. Im, A. Moritz, F. Steuber, V. Härle, F. Scholz, and A. Hangleiter, Appl. Phys. Lett. **70**, 631 (1997).

¹¹O. Brandt, H. Yang, and K. Ploog, Phys. Rev. B **54**, R5215 (1996).

¹²É. I. Rashba, Sov. Phys. Semicond. **8**, 807 (1975).

¹³O. Brandt, H.-J. Wünsche, H. Yang, J. R. Müllhäuser, R. Klann, and K. H. Ploog, J. Cryst. Growth **189/190**, 790 (1998).

¹⁴O. Brandt, K. Kanamoto, M. Gotoda, T. Isu, and N. Tsukada, Phys. Rev. B **51**, 7029 (1995).

¹⁵O. Brandt, in *III-V Quantum System Research*, edited by K. Ploog, Institution of Electrical Engineers (IEE), Materials and Devices Series 11 (Peregrinus, London, 1995), p. 70.